

By R. K. Moore, A. K. Fung, J. Young, J. Claassen, H. Chan, and M. Afarani, The University of Kansas Center for Research, Inc., Remote Sensing Laboratory, 2291 Irving Hill Drive, Lawrence, Kansas 66044, and W. J. Pierson, V. J. Cardone, J. Hayes, W. Spring, C. Greenwood, and R. Salfi, The University Institute of Oceanography of the City University of New York, N. Y. 10031*

ABSTRACT

The small-scale roughness of the sea surface is known to be in equilibrium with the local winds near the surface. Because radar backscatter and microwave emissions are sensitive to surface roughness, they are highly correlated with sea surface winds. The radiometric measurements are more sensitive than the backscatter measurements to variations in the atmosphere. The simultaneous collection of the two measurements permits most atmospheric effects to be removed from the data.

The S-193 Radscat made extensive measurements of many sea conditions. The equivalent 20 meter-elevation wind speeds range from calm to over 30 meters/sec. Measurements were taken in a tropical hurricane (Ava), a tropical storm (Christine), and in portions of extratropical cyclones. Approximately 200 scans of ocean data at 105 kilometer spacings were taken during the first two Skylab missions and another 200 during the final mission when the characteristics of the measurements changed due to damage of the antenna. More than 300 scans at 15 kilometer spacings show the finer spatial variation of winds. Backscatter with four transmit/receive polarization combinations (HH, VV, VH, HV) and emissions with horizontal and vertical receive polarizations were measured.

To correlate the Radscat measurements with surface winds, wind estimates (surface truth) were determined at each cell by objective numerical analysis techniques. These meteorological wind estimates are being analyzed to produce quantitative estimates of their accuracy. This analysis is necessary to relate the performance of microwave surface-truth wind estimator to the performance of a microwave true wind estimator. Results are not available at the time of writing.

Other surface parameters investigated for correlation with the measurements included sea temperature, air/sea temperature difference, and gravity-wave spectrum. The gravity-wave spectrum was estimated from numerical wave specification theories.

Methods were developed to correct the microwave measurements for atmospheric effects. The radiometric data were corrected accurately for clear sky and light cloud conditions only. The radiometer measurements were used to recover the surface scattering characteristics for all atmospheric conditions excluding rain. The radiometer measurements also detected the presence of rain which signaled when the scattering measurement should not be used for surface wind estimation. The ability of the system to operate successfully through clouds is important because clouds cover so much of the oceans.

Regression analysis was used to determine empirically the relation between surface parameters and the microwave measurements, after correction for atmospheric effects. Results indicate a relationship approaching square-law at 50° between differential scattering coefficient and wind speed with horizontally polarized scattering data showing slightly more sensitivity to wind speed than vertically polarized data. These results agree well with theory and show that sea surface winds can be measured accurately from space.

INTRODUCTION

Monitoring of meteorological conditions at sea has important applications which include global weather and wave forecasting, ocean circulation estimation, and severe weather tracking. Knowledge of sea-surface winds can be a valuable part of such a data system, particularly due to the close relation between pressure gradients and wind, and because surface winds are the inputs to wave forecasting programs.

An orbiting system which measures microwave backscatter and emissions from the sea can be used to map sea surface winds. Small-scale surface roughness increases with surface wind speed, and the microwave measurements are sensitive to this change in roughness.

Preliminary results of the analysis of S-193 Radscat microwave measurements over the sea are given here. The research is part of an effort to develop a system to measure sea-surface winds from space on a global basis.

BACKGROUND

Some of the more recent aircraft experimental measurements of backscatter as a function of wind speed are shown in Figures 1 a, b, and c. All of these observations were made near the incident angle range and frequency of the S-193 Radscat. Each shows a nearly linear relation between scattering coefficient in dB and the log of windspeed. A linear relationship between these is equivalent to having $\sigma^{\circ} = KW^{\alpha}$ where σ° is scattering coefficient and W is wind speed. The exponents, α , estimated from the NASA/JSC, NRL, and AAFE data range from 1 to 1.5 for incident angles from 25° to 65° and are shown in Figure 2. No clear trend with incident angle is evident from these data and the one-standard-deviation confidence intervals for the NRL data are rather large.

Figure 3 shows some experimental measurements of brightness temperature as a function of wind speed. The data show a linear trend between brightness temperature and wind speed for both 0° and 20° incident angle.

THE S-193 RADSCAT

The S-193 Radscat was a combined 13.9 GHz radiometer/scatterometer which operated aboard Skylab. The antenna beam was approximately circular with a two-way beamwidth of about 1.5° (scatterometer) and a one-way beamwidth of about 2° (radiometer). The scatterometer measured four polarizations (HH, VV, HV, VH) with both vertical and horizontal receive and transmit while the radiometer measured both vertically and horizontally polarized signals.

The modes designed for use over the sea sampled data at 105 kilometer intervals with incident angles of approximately 50°, 40°, 30°, 15°, and 0°. A scan in these modes consisted of four scattering coefficients and two radiometric measurements at each of the five incident angles. Approximately 200 such scans of ocean data were taken during the first two Skylab missions and an additional 200 during the final mission. Backscatter data from the final mission require special processing to partially compensate for the effects of a damaged antenna feed. The radiometric measurements during the final mission are believed to be of little value because of the damage. The results presented here are based on the preliminary analysis of about 25% of the scans obtained during the first two Skylab missions. The analysis of the remainder of data from these missions awaits processing to determine surface truth. Preliminary evaluation of backscatter data from the final Skylab mission indicates that the wind sensitivity of the data was not destroyed by the antenna damage, but these data must still be corrected for the effects of the antenna damage.

The S-193 Radscat also operated in a mode which observed a contiguous two-dimensional array of cells on the surface. The nominal distance between centers of these cells was 13.5 km. Data obtained in this mode can be used to form maps which show the finer spatial variations in the surface winds.

THE AAFE RADSCAT UNDERFLIGHTS

The Advanced Application Flight Experiment program, AAFE, included an aircraft-mounted Radscat capable of measurements similar to those of the S-193 Radscat. This instrument had been operated before the launching of Skylab to measure the wind dependence of backscatter and brightness temperature, but only a limited number of wind speeds were observed by the system (see Figure 1c).

Several AAFE Radscat flights were flown concurrently with the S-193 Radscat operation to compare measurements of the two instruments. The AAFE measurements also give an indication of the fine spatial variations of the return because the area illuminated by the AAFE antenna pattern is much smaller and the measurements are separated by a shorter distance than those of the S-193.

The most important measurements by the AAFE instrument were obtained when the aircraft on which the instrument was mounted flew in a tight circle, an experiment mode designed by W. L. Jones of NASA/LRC. During this maneuver, the AAFE Radscat takes measurements at about 30° incident angle with the azimuthal direction changing continuously. The averaged values of backscatter for four continuous circles are shown in Figure 4. The highest scattering coefficients were measured when the instrument

was pointing upwind, in the direction from which the wind was blowing. A secondary maximum occurs for downwind with minima near crosswind. Some of the scatter in the data is caused from both temporal and spatial variations in the wind field. The solid curve indicates the fit of the first four terms of a Fourier series. Perhaps additional terms need to be added to the model to better fit the minima.

The difference between upwind and crosswind for the 3 m/sec wind speed data shown is about 2.5 dB with about 1 dB difference between upwind and downwind. Data taken for 12 m/sec winds and 40° incident angle indicate about a 6 dB difference in vertically-polarized scattering coefficient between upwind and crosswind. A higher wind speed case has recently been measured, but the processing of these data is not completed.

These data give an indication of the sensitivity of backscatter measurements to wind direction, but data are available for only a few wind speed/incident angle/wave spectra combinations. Furthermore, no data are available to document the effects of wind direction on cross-polarized measurements. To fill in these gaps, we must presently rely on theory. A theory has been developed to explain and extend these results, but results are not given here because estimates of wave slopes used in the theory are being revised.

PRELIMINARY ANALYSIS OF S-193 RADSCAT DATA

The S-193 Radscat measured microwave responses through tropical hurricane Ava and tropical storm Christine. These were the first measurements of ocean backscatter during such storms. The instrument was scanning to one side of the track during both storms and during Christine the instrument measured cells in all four quadrants of the storm. Measurements during Ava have been reported previously.^{4,5}

Figure 5 shows the passive and active microwave response as the spacecraft passed by Christine. The figure also shows the wind profile calculated from a meteorological model⁶ that uses as inputs central pressure, radius to maximum wind, ambient pressure, and direction and speed of movement of the eye. Unfortunately, the aircraft reconnaissance flights closest to the time of the Skylab pass were 2 hours before and 6 hours after the pass. Both were at an altitude of 3000 meters. For these reasons, the location of the eye at the time of the Skylab pass is uncertain. Even so, Figure 5 shows good correlation between backscatter and windspeed. The surface truth wind speed peaks at scan 10 while the scattering coefficients remain high from scan 10 through scan 12 or 13. This could be the result of the wind peak not being as sharp as indicated by the wind models. Secondary peaks in wind speed often occur in such storms.

The high apparent temperature at scan 13 indicates the presence of heavy rain. In such cases, the scatterometer receives substantial backscatter from the rain drops and should, therefore, not be used to estimate surface wind speed.

Several data segments over the sea were observed by the S-193 in a mapping mode. Figure 6 shows the backscatter and apparent temperatures which were measured southeast of Vietnam. Twelve measurements were taken in the cross-track dimension which is the narrow dimension of the images. The upper four images are of the South China Sea and the lower four are of the Flores Sea (south of Borneo). The left two images of each sea show different ranges of scattering coefficients and the right two show apparent temperature. Thresholds for the printing were set differently for a than for b, and for c than for d.

The left-most image of each sea, a, identifies the land-sea boundaries from the backscatter. The c apparent temperature images can next be used to identify the location of rain. Note the two rain bands about 160 and 260 kilometers north of and parallel to the Borneo coast. Additional rain patches are near Vietnam. The high apparent temperatures over the sea indicated in images d show the areas of thick cloud cover. A front appears to be present north of Borneo. The winds may be inferred from the backscatter from ocean areas not experiencing rain. The wind sensitive measurements may be seen in images b. The backscatter north of the front is 4 to 6 dB higher than that south of the front. This difference could be due to a change in wind speed, but much of the difference is probably due to a change in direction which is usually associated with such fronts. The winds along the northern coast of Borneo are probably cross-wind w.r.t. the instrument and those to the north of the front are more up or down wind. Figure 7 shows the same area with the levels of scattering coefficient and apparent temperatures distinguished by color enhancement. The surface truth for this area is currently being compiled.

The wind speed dependence of the backscatter data at 40° incident angle is indicated in Figures 8, 9, and 10. The points shown in these figures represent about 25 per cent of the data collected during the first two Skylab missions and are those for which preliminary surface truth is available. The data were taken at many different aspect angles relative to wind direction. Because backscatter can vary by as much as 6 dB due to aspect angle differences, an aspect angle correction based on an AAFE circle flight has been applied to the like-polarized data shown in Figures 8 and 9. It should be noted, however, that the scatter of the points in Figures 8 and 9 was not substantially reduced by applying the aspect angle correction. Furthermore, when a linear function of log wind speed was fit to the measured values in dB, the residuals of the fit plotted versus aspect angle did not display any significant trend. These results may be due to inaccurate meteorological wind estimates or simply to the limited size of the data set. For whatever reason, the aspect angle corrections currently applied to these data have questionable validity.

The nearly linear trend between scattering coefficient in dB and log wind speed is clearly evident in each of the three figures. The scatter in the data is greater than one might like; however, much of the scatter is due to uncertainties in the surface truth wind speed. The surface truth values are calculated using pressure and wind measurements from ships and planes in the area. Often there are no sources of the meteorological measurements close in time or space to the Radscat measurements. Even with measurements close to the Radscat cells, the surface truth wind speeds may have an r.m.s. error of 2 m/sec or greater. A quantitative evaluation of the accuracy of the surface truth is underway to identify the portion of scatter in the data due to surface truth errors.

Measurements made with the AAFE Radscat during one of the Gulf of Mexico passes showed very close agreement with both S-193 data and local wind speed measured from the aircraft.⁷ These values of wind speed were significantly different from those given by the meteorological analysis used here and based on observations at points far from the Radscat observation cells. This lends considerable credence to the hypothesis that much of the scatter is due to inaccurate knowledge of surface conditions from meteorological analysis. In other words, "surface truth" often is not very "true"!

The preliminary power law trends indicated by the S-193 data analyzed to date are shown in Figure 11. The exponents of wind speed range from close to 1.5 to just over 2 with horizontally polarized data having a slightly larger exponent than vertically polarized for the two highest incident angles. The increase of the exponent with incident angle is clearly indicated while such a trend was not apparent in the data shown in Figure 2. This increase with incident angle was predicted in previous work on the basis of the small-perturbation theory and latest estimates of the capillary part of the wave spectrum.

CONCLUSION

Measurements with the S-193 radiometer/scatterometer have confirmed the strong relationship between scattering coefficient for microwave backscatter and the surface winds on the sea. The sensitivity appears to be somewhat greater than that shown in earlier aircraft measurements, but is in line with the results of AAFE Radscat underflight experiments. Sensitivity is somewhat greater for horizontal than for vertical polarization at the higher angles, with cross-polarized results giving essentially the same sensitivity as horizontally polarized.

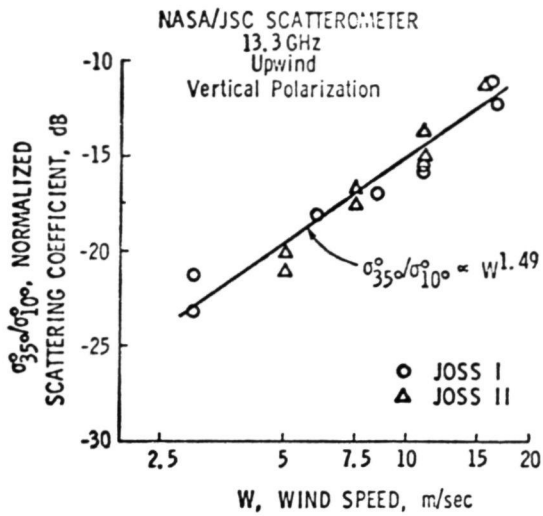
During Hurricane Ava and tropical storm Christine, measurements were made in high winds and during the occurrence of heavy rain. The ability of the radiometer to detect the presence of the rain and thereby to warn that the scatterometer results are questionable or should be corrected was demonstrated.

Because of late arriving data, surface truth computations for most Skylab passes have not yet been combined into the analysis, so the results presented here are based on two passes during relatively calm weather and the two large storms. The surface truth data are now available, and at the time of writing were in the process of being combined with the Skylab data. Extensive measurements were made in the North Atlantic during SL-4, and the especially processed data (degraded because of antenna damage) are just becoming available at the time of writing.

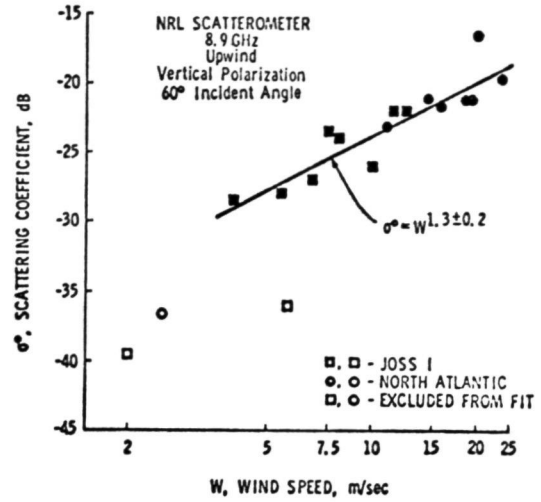
Use of the Cross-Track-Contiguous mode of the S-193 permits observation of moderately fine scale variations in the surface wind structure, as well as the rain structure. Although analysis of these data is just commencing, two interesting examples have been presented here to illustrate the type of variation encountered.

REFERENCES

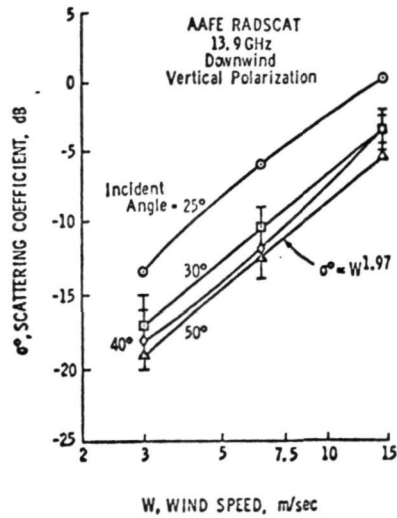
1. Bradley, G.A., "Remote Sensing of Ocean Winds Using a Radar Scatterometer," Ph.D. Thesis, University of Kansas Center for Research, Inc., September, 1971.
2. Moore, R. K., J. P. Claassen, A. K. Fung, S. Wu, and H. L. Chan, "Toward Radscat Measurements Over the Sea and Their Interpretation," in Advanced Applications Flight Experiments Principal Investigators' Review, NASA Langley Research Center, October, 1971, pp. 115-140.
3. Jones, W. L. et al., IEEE Intercon Technical Papers, IEEE International Convention and Exposition, Session 34, Ocean Physics Applications Program, March 26-29, 1974.
4. Cardone, V. J., R. K. Moore, W. J. Pierson, and J. D. Young, "Preliminary Report on Skylab S-193 Radscat Measurements of Hurricane AVA," The University of Kansas Center for Research, Inc., Remote Sensing Laboratory, Technical Report 254-1, October, 1973.
5. Moore, R. K., J. P. Claassen, A. C. Cook, D. L. Fayman, J. C. Holtzman, A. Sobti, W. E. Spencer, F. T. Ulaby, J. D. Young, W. J. Pierson, V. J. Cardone, J. Hayes, W. Spring, R. J. Kern, and N. M. Hatcher, "Simultaneous Active and Passive Microwave Response of the Earth--The Skylab Radscat Experiment," Presented at the 9th International Symposium on Remote Sensing of Environment, Ann Arbor, Michigan, 15 April, 1974.
6. Chow, Shu-Hsien, "A Study of the Wind Field in the Planetary Boundary Layer of a Moving Cyclone," New York University Department of Meteorology and Oceanography, (M.S. Thesis), 1971.
7. Jones, W. L., personal communication.



(a) - ref. 1.



(b) - ref. 2.



(c) - ref. 3.

Fig. 1. MEASURED WIND SPEED DEPENDENCE OF SCATTERING COEFFICIENTS

MODEL: $\sigma^{\circ} = KW^{\alpha}$

where σ° is scattering coefficient
 W is wind speed

○	NRL	8.9 GHz	(3.4 cm)	upwind
□	NASA/JSC	13.3 GHz	(2.25 cm)	upwind
△	AAFE	13.9 GHz	(2.16 cm)	downwind



Error bars indicate ± one estimated standard error
 (No estimated standard errors are available for the AAFE data)

Fig. 2. EMPIRICAL ESTIMATES OF THE POWER LAW RELATING WIND SPEED AND VERTICALLY POLARIZED SCATTERING COEFFICIENTS

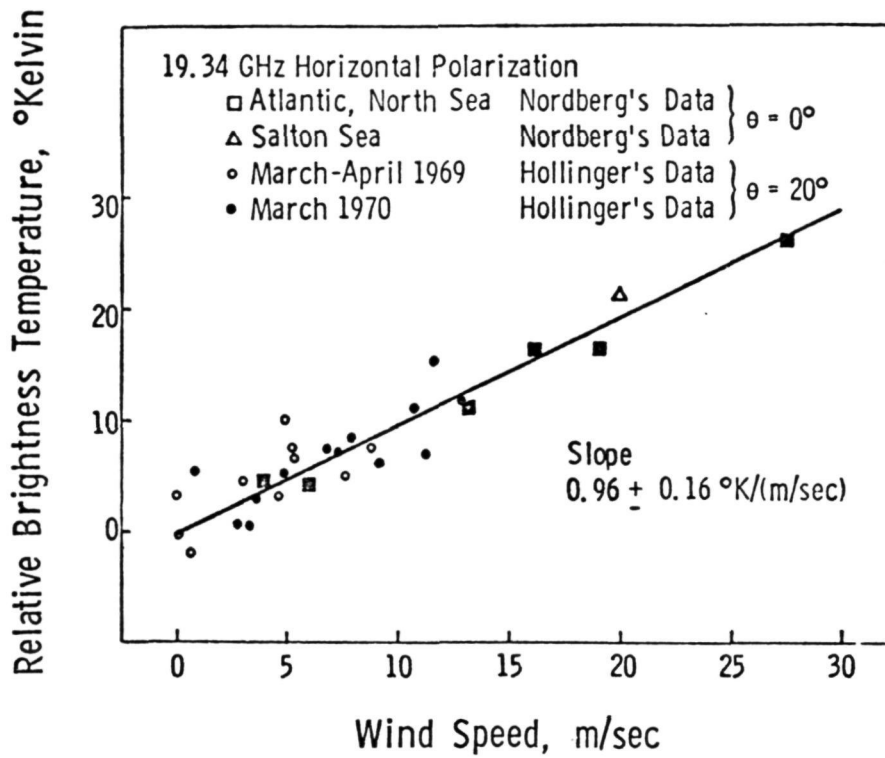


Fig. 3. Correlation between Radiometric Brightness Temperature of the Sea and Surface Wind Speed. Ref. 2.

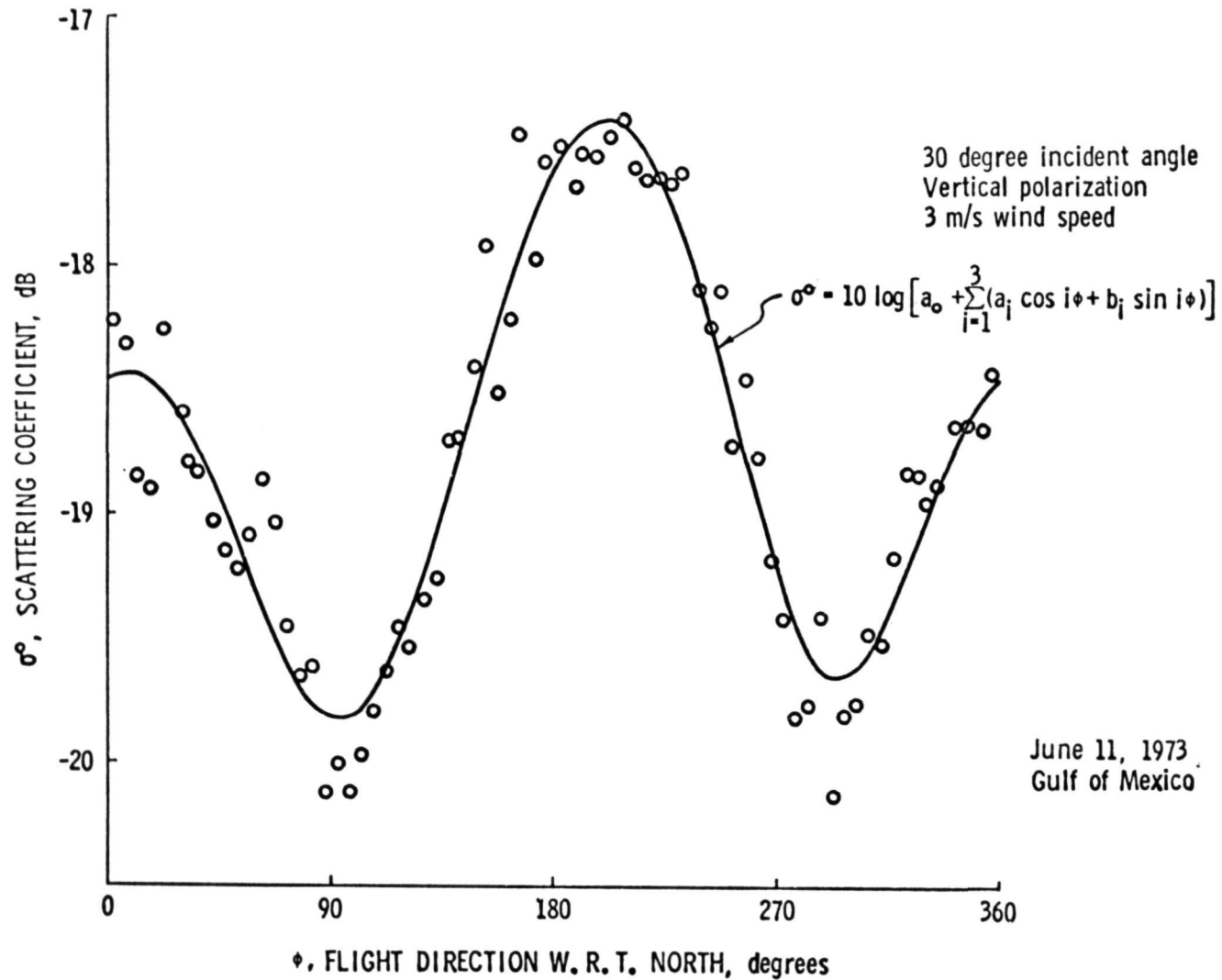


Fig. 4. MEASURED WIND DIRECTION DEPENDENCE OF SCATTERING COEFFICIENTS

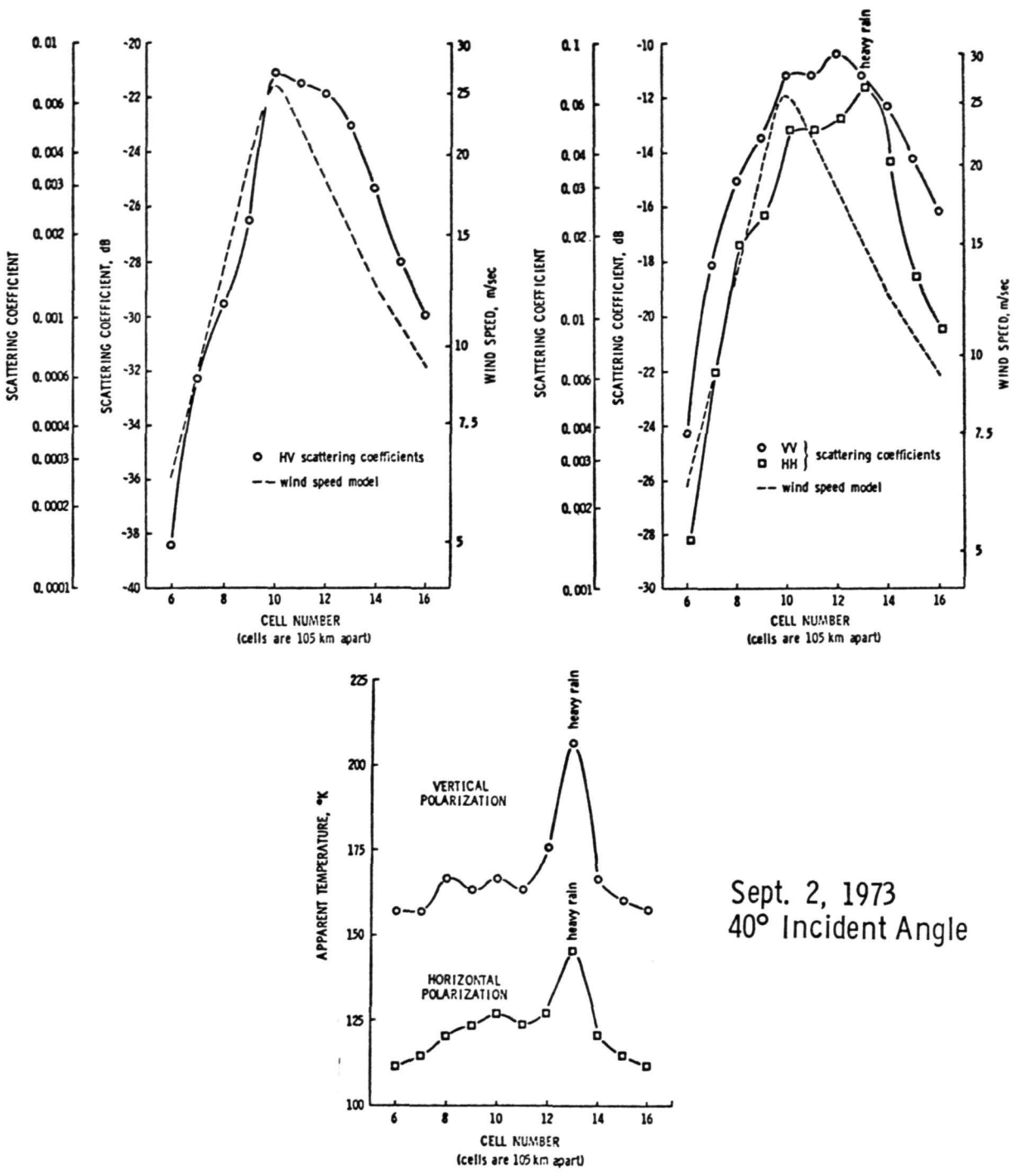
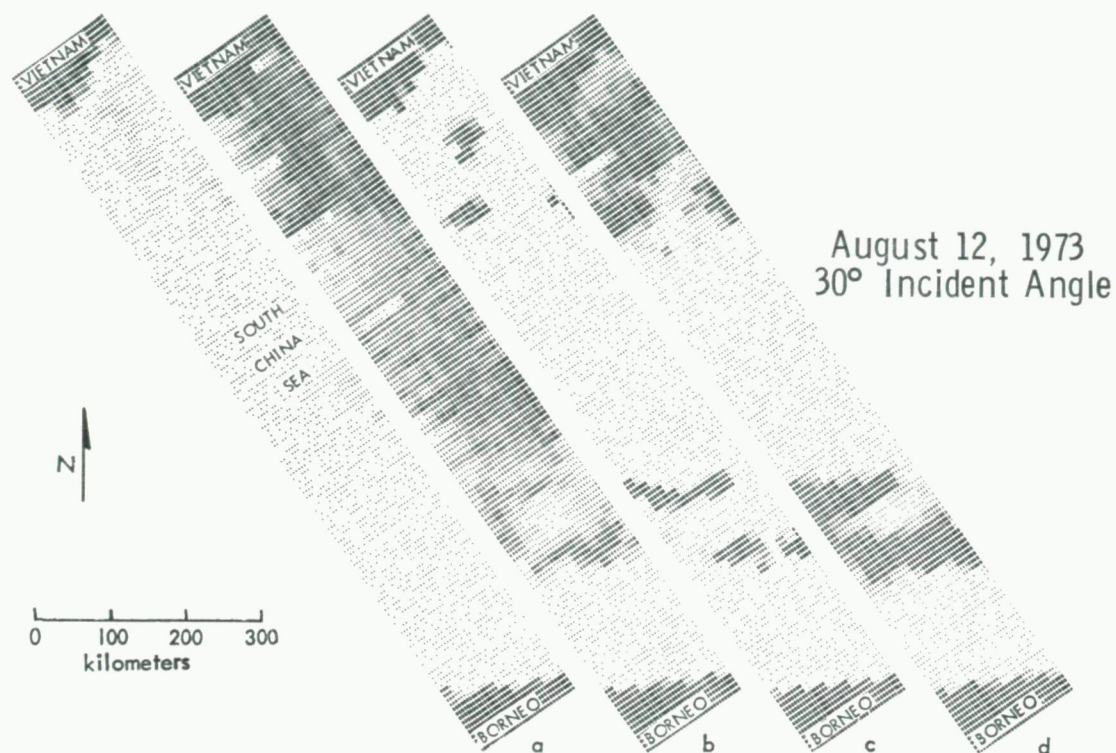




Fig. 5. SCATTERING AND RADIOMETRIC RESPONSES OF TROPICAL STORM CHRISTINE



EXTREMES	a	b	c	d
	$\sigma_{HH}^{\circ} > -6 \text{ dB}$ land	$\sigma_{HH}^{\circ} > -10 \text{ dB}$ land or rain or sea surface winds such as: upwind > 9 m/s crosswind > 13 m/s	$T_H > 170^{\circ} \text{ K}$ land or rain	$T_H > 150^{\circ} \text{ K}$ land or rain or heavy clouds
	$\sigma_{HH}^{\circ} < -11 \text{ dB}$ sea	$\sigma_{HH}^{\circ} < -15 \text{ dB}$ sea surface winds such as: upwind < 6 m/s crosswind < 8 m/s	$T_H < 160^{\circ} \text{ K}$ sea	$T_H < 130^{\circ} \text{ K}$ clear or light clouds over sea

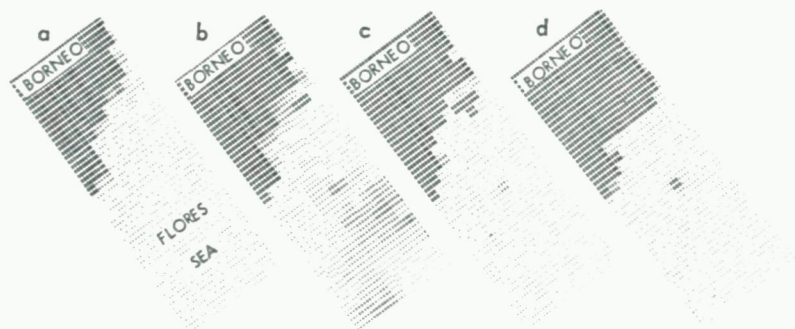


FIG. 6. SCATTERING AND RADIOMETRIC RESPONSES FROM THE SOUTH CHINA AND FLORES SEAS

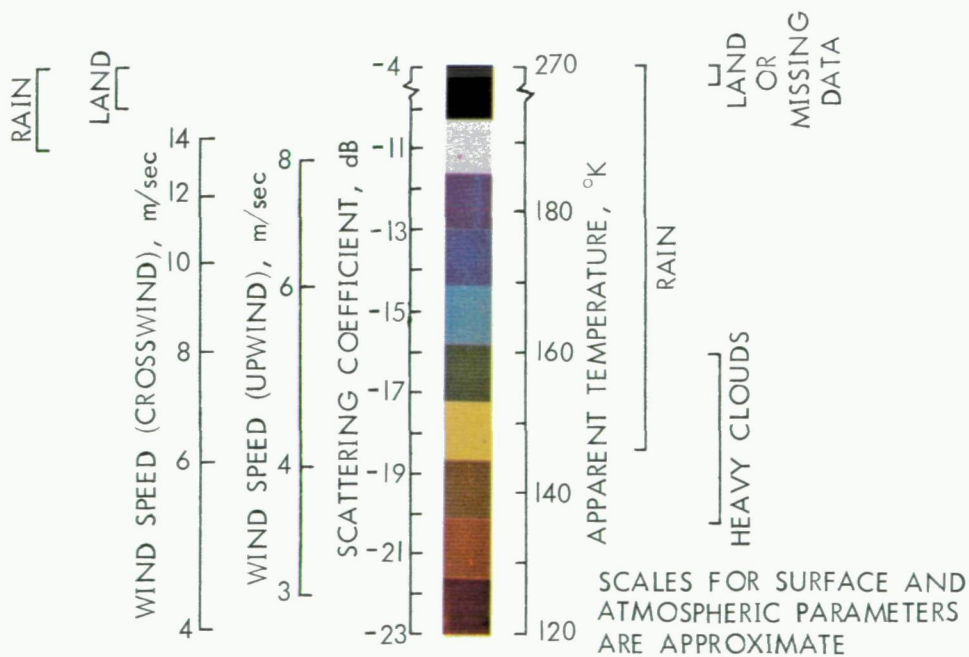
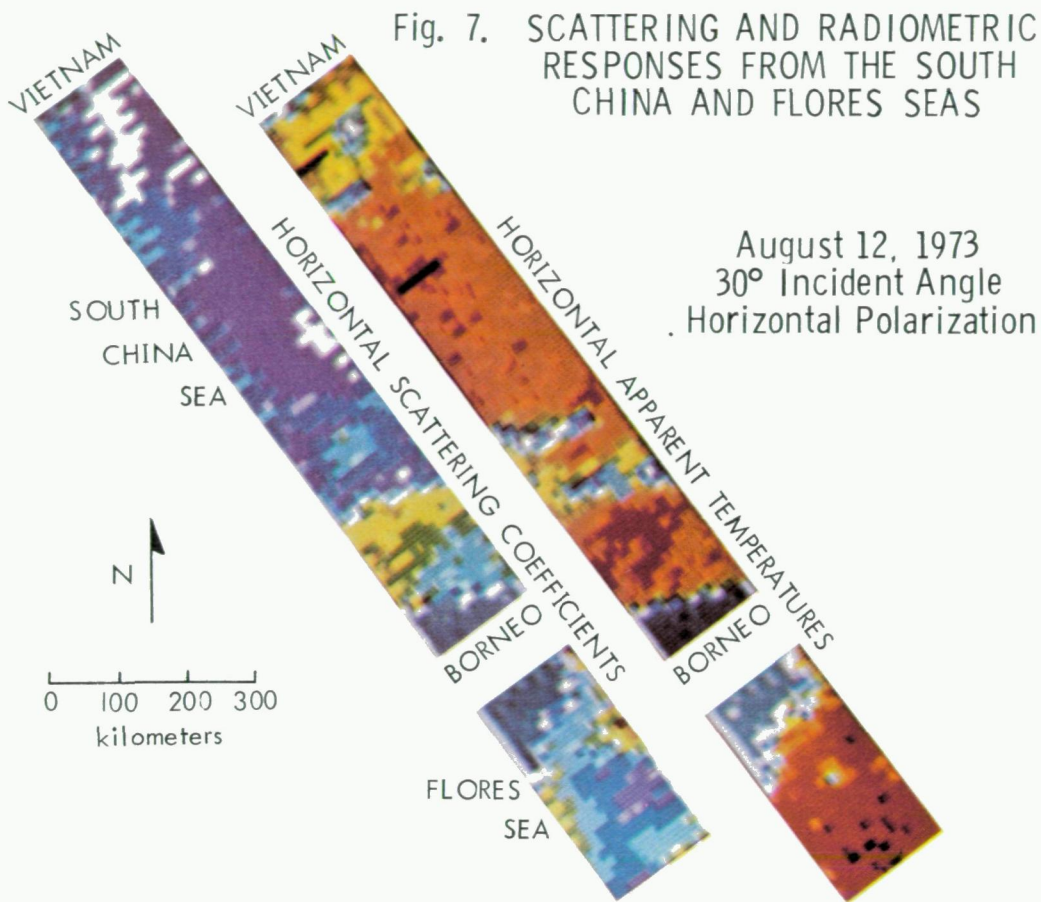


FIG. 7. SCATTERING AND RADIOMETRIC RESPONSES FROM THE SOUTH CHINA AND FLORES SEAS

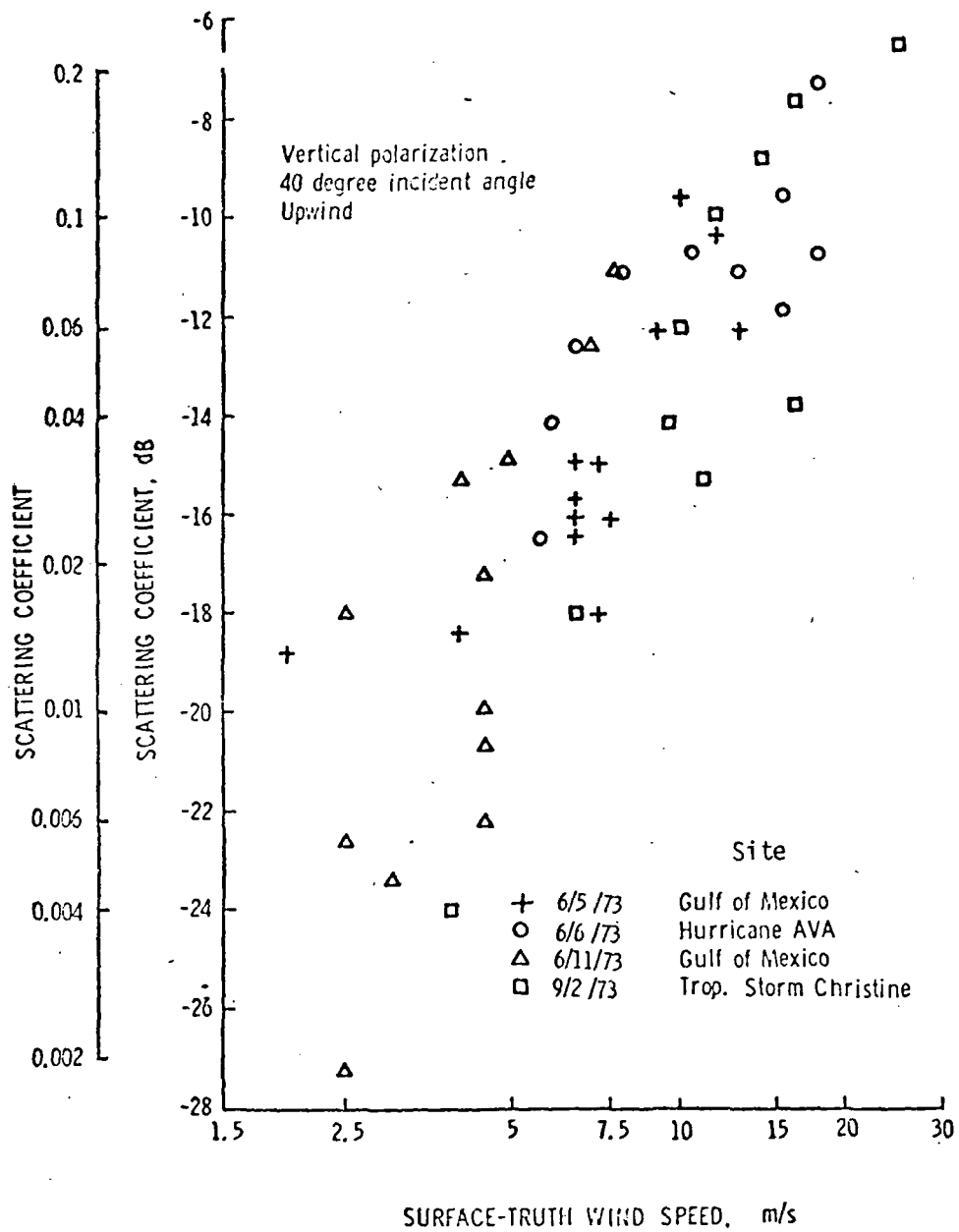


FIG. 8. WIND SPEED DEPENDENCE OF SCATTERING COEFFICIENTS (PRELIMINARY), VERTICAL POLARIZATION

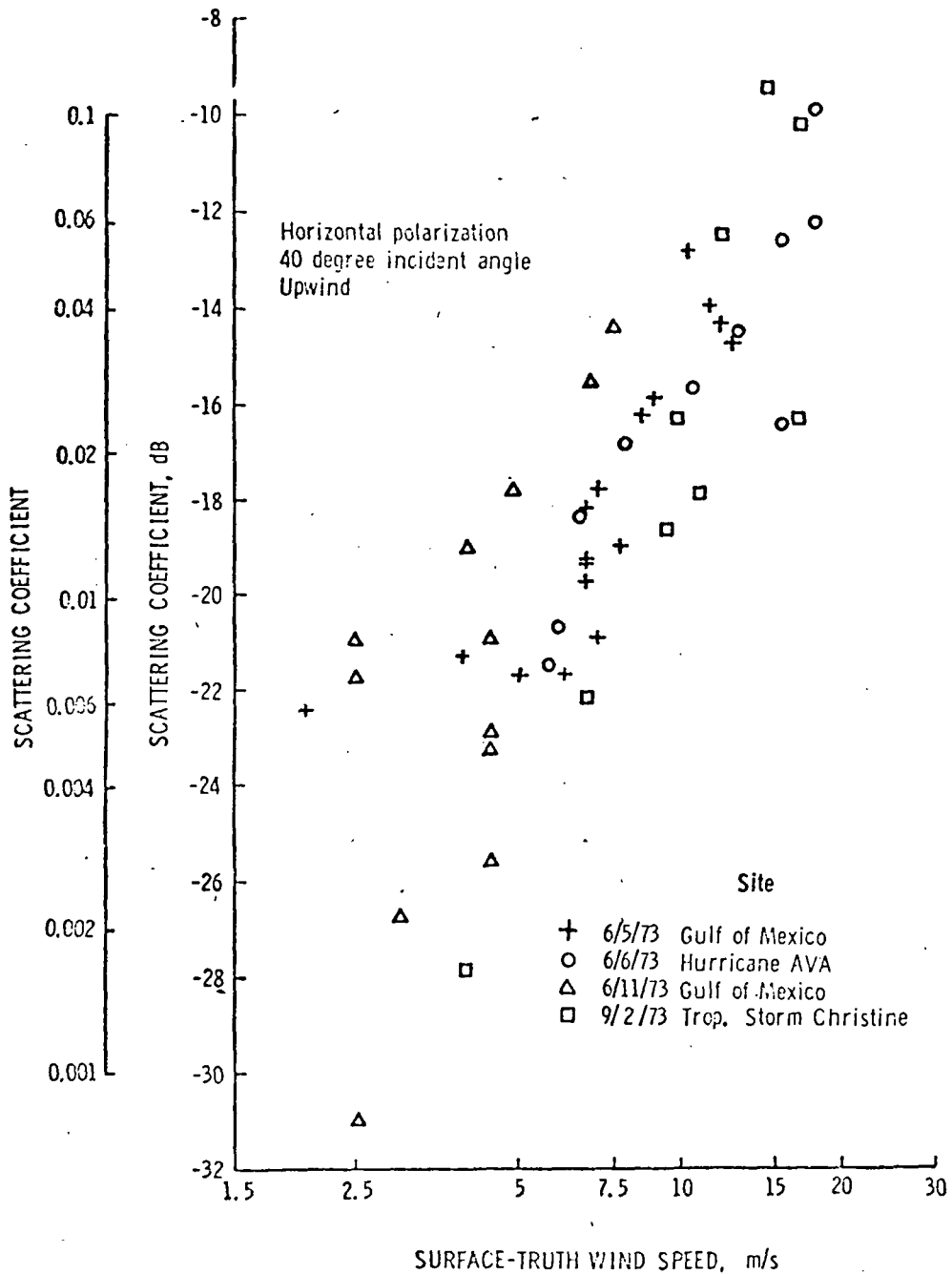


FIG. 9. WIND SPEED DEPENDENCE OF SCATTERING COEFFICIENTS (PRELIMINARY), HORIZONTAL POLARIZATION

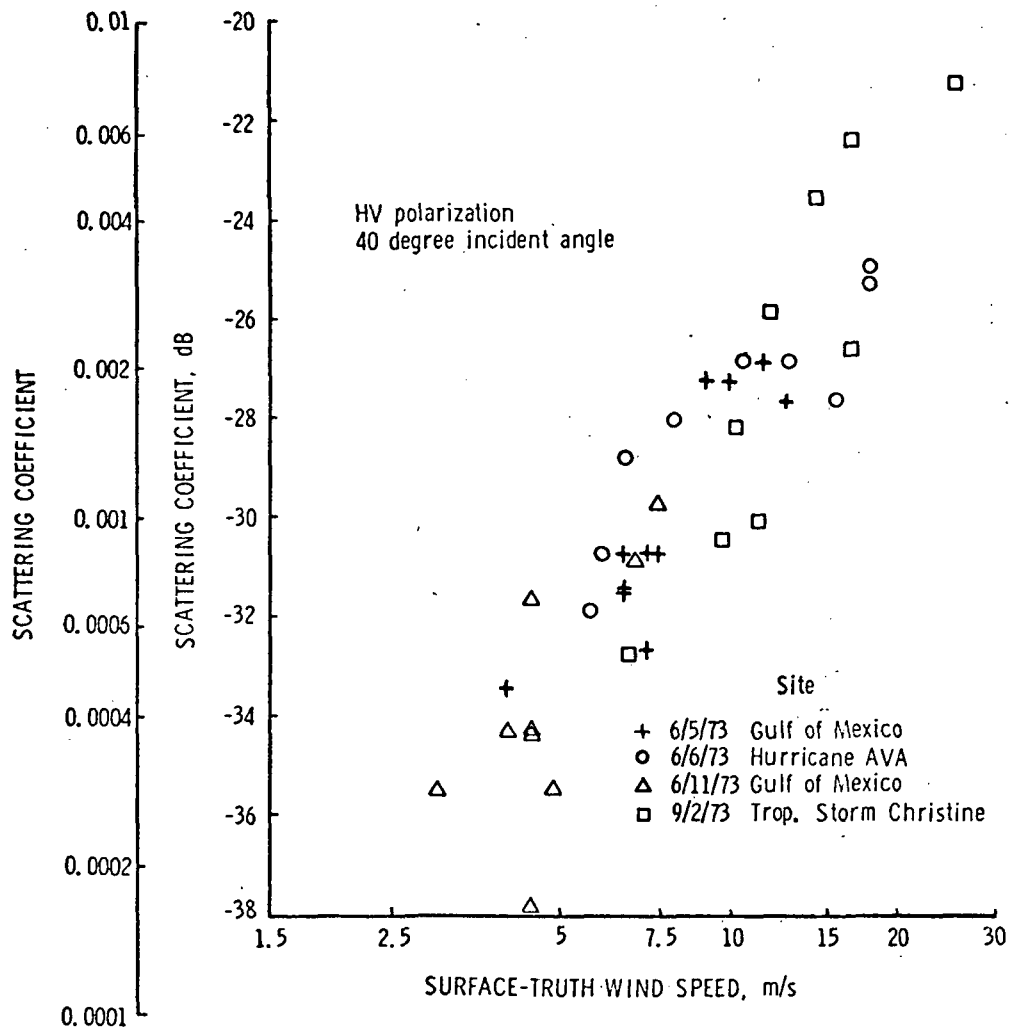
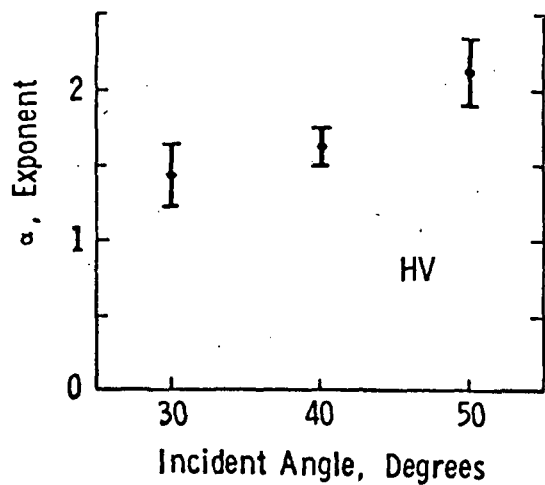


FIG. 10. WIND SPEED DEPENDENCE OF SCATTERING COEFFICIENTS (PRELIMINARY), HV POLARIZATION



Model: $\sigma^\circ = k w^\alpha$

where σ° is scattering coefficient
 w is wind speed

Error bars indicate \pm one estimated standard error

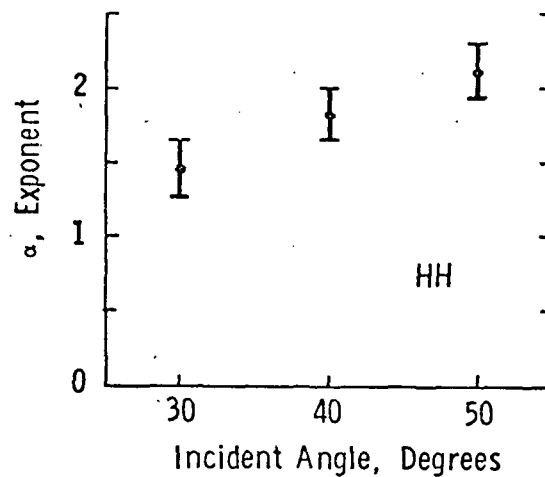
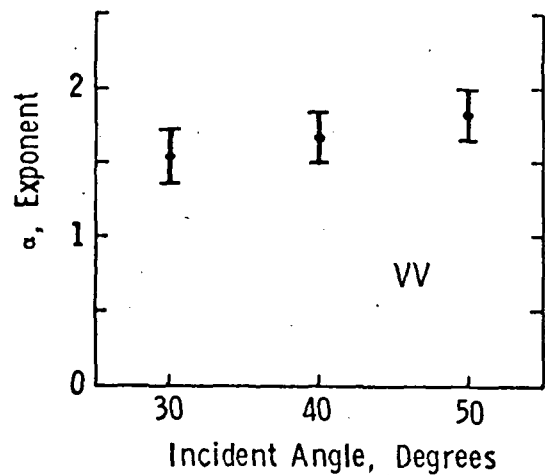


Fig. 11. Preliminary empirical estimates of the power law relating wind speed and scattering coefficient at 13.9 GHz (2.16 cm wave length)